JOURNAL OF SOLID STATE CHEMISTRY 116, 335–342 (1995)

"$Nb_{2-x}P_{3-y}O_{12}$," a Novel Nb^{V} Oxophosphate with Disordered Cation Vacancies in a $Sc_2(WO_4)_3$-Type Structure

J. J. Zah-Letho,*,† A. Verbaere,†,[1] A. Jouanneaux,† F. Taulelle,‡ Y. Piffard,† and M. Tournoux†

*Laboratoire de Chimie Minérale, Faculté des Sciences et Techniques, 22 BP 582, Abidjan 22, Republic of the Ivory Coast;
†Laboratoire de Chimie des Solides, UMR n° 110 CNRS, Université de Nantes, 2, rue de la Houssinière, 44072 Nantes Cedex 03, France;
‡Laboratoire de RMN, Institut de Chimie, Université Louis Pasteur, 2, rue Blaise Pascal, 67000 Strasbourg, France

Received February 4, 1994; in revised form September 19, 1994; accepted November 10, 1994

The title compound was prepared at 360°C, starting from Nb_2O_5 and $NH_4H_2PO_4$. The orthorhombic unit-cell parameters were determined by electron and X ray diffractions: a = 12.0819 (2) Å, b = 8.6848 (1) Å, c = 8.7452 (1) Å, space group *Pbcn*. Rietveld refinements from X ray powder diffraction data, chemical analyses, and the measured density show that the basic structure consists of a three-dimensional framework of the $Sc_2(WO_4)_3$ structure type, with NbO_6 octahedra and PO_4 tetrahedra sharing corners, and that both Nb and P vacancies occur. The actual formula is close to $Nb_{2-x}P_{3-y}O_{12}$. Comparative spectroscopic studies of the title compound and of $Nb_3(NbO)_2(PO_4)_7$ confirm the occurrence of the vacancies, and thus an important local variation of the bond lengths near the defect sites. The presence of small amounts of H and N in the structure is discussed. Upon heating in air, the structure is preserved up to 900°C. The so-called ε-$NbOPO_4$ has the same basic structure, and its existence seems questionable.

INTRODUCTION

In the course of attempts to prepare phosphatoniobic acids as ion-exchangers, the title compound was obtained. Its X ray powder diffraction (XRPD) pattern is rather similar to that reported earlier for $NbP_3O_{10} \cdot 2H_2O$ (1), and very similar to that of the compound previously named ε-$NbOPO_4$ (2). The XRPD data, however, strongly suggest a structure closely related to the $Sc_2(WO_4)_3$ type, which implies a $M_2(PO_4)_3$ covalent framework. M is an octahedral cation, with a mean oxidation number of 4.5, whereas the title phosphate involves Nb^{V}; it has therefore a defect $Sc_2(WO_4)_3$ structure.

This paper reports on the preparation, composition, and structure of the title compound. A plausible structural model for the defects, supported by spectroscopic studies, is proposed. A discussion of the existence of ε-$NbOPO_4$ is given.

PREPARATION

$NH_4H_2PO_4$ and Nb_2O_5 were weighed out in the atomic ratio Nb : P of 1 : 3, ground and mixed. The mixture was heated in a platinum crucible, in air, up to 360°C, and held at this temperature for 30 hr. The heating rate must be at least 2 K/mn, in order to prevent the formation of significant amounts of $Nb_3(NbO)_2(PO_4)_7$ (3).

After cooling, the product was washed repeatedly with water, ethanol, ether, and acetone in turn, to remove the excess phosphorus oxide, and dried in an oven at 100°C before final heating at 400°C for 15 hr. The product is a white, finely divided, crystalline powder.

XRPD patterns of unsieved samples do not exhibit any impurity lines. However, sieved samples are required for data collection in view of Rietveld refinements, and their XRPD pattern shows a few weak supplementary lines arising from very small amounts of Nb_2O_5 and $Nb_3(NbO)_2(PO_4)_7$. It appears that sieving increases the impurity level in the resulting powder, likely in relation with their relative particle size; however the impurity level in such samples remains very low.

CHEMICAL COMPOSITION

The values of the Nb : P atomic ratio, obtained by energy dispersive spectrometry using a JSM 35C microscope, are 1 : 1.50 ± 6%. For these determinations, $NH_4NbOP_2O_7$ (4) and α-$NbOPO_4$ were used as standards, and several microcrystals were studied in each case.

Quantitative analyses were performed at the Service Central d'Analyse du CNRS (Vernaison, France). They lead to (in percentage by weight)

Nb: 38.8 P: 19.1 N: 0.35 H: 0.13.

The hydrogen content is very low and therefore very imprecise, but the result is reproducible. The small nitrogen content was also obtained by using the method de-

---

[1] To whom correspondence should be addressed.

0022-4596/95 $6.00

TABLE 1
XRPD Data for the Title Compound

h k l	d_{calc} (Å)	I/I_0	*h k l*	d_{calc} (Å)	I/I_0
2 0 0	6.041	4	4 2 2	2.157	8
1 1 1	5.490	18	1 4 1	2.076	5
0 0 2	4.372	38	0 2 4	1.953	7
0 2 0	4.342	44	2 3 3	1.945	20
2 1 1	4.314	100	1 2 4	1.928	6
0 2 1	3.889	13	3 0 4	1.921	5
1 1 2	3.716	26	6 1 1	1.914	20
1 2 1	3.702		5 2 2	1.901	5
3 1 0	3.653	24	3 3 3	1.830	5
3 1 1	3.371	11	6 0 2	1.829	
2 1 2	3.279	14	3 2 4	1.757	6
0 2 2	3.081	48	4 3 3	1.699	7
4 0 0	3.020	20	2 1 5	1.649	5
1 2 2	2.985	8	4 2 4	1.640	25
1 3 0	2.815	4	2 5 1	1.640	
4 1 1	2.712	4	4 4 2	1.635	10
1 1 3	2.694	14	6 1 3	1.627	12
2 1 3	2.513	17	6 3 1	1.624	12
2 3 1	2.502	26	0 4 4	1.541	5
4 0 2	2.485	23	1 4 4	1.528	4

Note. Reflections with $I/I_0 < 4$ are not given.

scribed in (5), for oxonitrides. The atomic ratio Nb : P (1 : 1.48) agrees well with the above mean value of 1 : 1.50 obtained for individual microcrystals. The ratio 1 : 1.48 ± 4% was retained for the structural study.

Magnetic susceptibility measurements performed in the temperature range 80–300 K show a diamagnetic behavior, as expected for this white niobium compound. One can conclude that the oxidation number of Nb is V.

As will be seen later, MAS NMR spectra indicate that protons are present in the compound in a variety of states, in agreement with the TG curves. The studies make it possible to mainly distinguish between protons in H_2O, loosely bonded at the surface, and those in the bulk (ca. 18 and 82%, respectively). The composition in the bulk is therefore

$$\text{Formula I, } Nb_2P_{2.96}O_{12.4}N_{0.12}H_{0.5},$$

where the hydrogen content is very imprecise.

UNIT-CELL PARAMETERS AND CONTENT

The XRPD pattern of the title compound (Table 1) is very similar to that of $(Sb^{III}_{1/2}Nb_{3/2})(PO_4)_3$, which is of $Sc_2(WO_4)_3$ structure type (6, 7). The unit-cell parameters, refined from the XRPD data, are given in Table 2. The structure type corresponds to an $M_2X_3O_{12}$ formula, with $Z = 4$ (M = octahedral cation, X = tetrahedral cation). Comparison with formula I clearly shows that defects must occur, in the present case, in an $M_2(XO_4)_3$ framework, either with vacancies, or ion excess (or both).

An electron diffraction study, conducted in a JEOL 100 CX microscope, confirmed the periodicity of the lattice and revealed the absence of diffuse intensity associated with partial order.

The value of the density, measured by the pycnometric method for two samples, is $d = 3.244$ g.cm^{-3}, which is significantly lower than the theoretical value (3.407) associated with the $Nb_2P_3O_{12}$ (nonneutral) formula. Thus, cation vacancies (at least) must occur in the $Nb_2P_3O_{12}$ framework.

It must be noted that the low impurity content cannot significantly affect the experimental density, since the density of the major impurity, $Nb_3(NbO)_2(PO_4)_7$, is 3.372, i.e., only 4% higher than the measured value.

The experimental density is usually found slightly lower than the theoretical one by one or a few percent, so that the formula weight should be in the range from 448.2 to about 460 g, neglecting the very low possible contribution of superficial H_2O to the density obtained. The following formula,

$$\text{Formula II, } Nb_{1.91}P_{2.82}H_{0.5}(O_{11.89}N_{0.11}),$$

corresponds to 457.2 g. Although it can be discussed, this formula was retained, as it takes all results into account and contains 12 anions (O and N). Other slightly different formulas could be proposed, for instance, with both cation and anion vacancies. In these cases, the Nb and P content would not be greatly modified.

Formula II leads to Nb vacancies (4.5%) and P vacancies (6%) in an $Nb_2(PO_4)_3$ framework. For simplification,

TABLE 2
Crystallographic Data and Refinement Results

Formula for the refinement	$Nb_{1.91}P_{2.82}O_{12}$	Space group	*Pbcn*
Z	4	a (Å)	12.0819(2)
b (Å)	8.6848(1)	c (Å)	8.7452(1)
V (Å^3)	917.63(3)	Counting time (hr)	15
Angular range (2θ°)	13.4–111.5	Number of data	3224
R factors (%) R_I	4.4	Number of reflections	615
R_{wp}	5.8		
R_{exp}	1.3		

Atom	Occupancy (%)	x	y	z	B (Å^2)
Nb	95.5	0.3812(1)	0.2504(3)	0.4665(1)	0.85(4)
P(1)	94	0.	0.4690(8)	0.25	1.10(9)
P(2)	94	0.3556(4)	0.3929(6)	0.1146(5)	"
O(1)	100	0.144 (1)	0.071 (1)	0.095 (1)	1.1 (1)
O(2)	100	0.0657(8)	0.362 (1)	0.148 (1)	"
O(3)	100	0.2716(8)	0.319 (1)	0.006 (1)	"
O(4)	100	0.4185(7)	0.068 (1)	0.340 (1)	"
O(5)	100	0.4671(8)	0.324 (1)	0.066 (1)	"
O(6)	100	0.3281(9)	0.356 (1)	0.279 (1)	"

formula II has been approximated here to "Nb_{2-x}-$P_{3-y}O_{12}$," as a name for the title compound.

STRUCTURE REFINEMENT

XRPD data were collected using an INEL multidetector system, and Cu$K\alpha_1$ radiation. The sample was sieved at 10 μm and placed in a glass Lindemann capillary of 0.2 mm diameter. As already mentioned, the pattern shows a few lines arising from a very small amount of both Nb_2O_5 and $Nb_3(NbO)_2(PO_4)_7$ as impurities. The lines from the minor impurity, Nb_2O_5, were eliminated by excluding a few 2θ regions from the refinement. It must be mentioned that these supplementary lines appear only after a very long exposure required for the improvement of the signal to noise ratio. Those from $Nb_3(NbO)_2(PO_4)_7$ were accounted for using the data previously given for this phase (3) and refining the scale factor only.

For the Rietveld refinement, the GSAS program (8) was used, with seven pseudo-Voigt profile parameters, 10 Fourier coefficients for the background, and four parameters for the line positions (*a, b, c,* and zero point). The program calculates R_{wp} and R_{exp} values which include the background. The initial atomic parameters were taken from those in $(Sb^{III}_{1/2}Nb_{3/2})(PO_4)_3$ (6), with space group *Pbcn*. The probable occurrence of N substituted at the O sites was neglected. An overall isotropic thermal B parameter was applied to each kind of atom. The absorption coefficient was adjusted in order to obtain positive B values for all atoms.

The first refinement, performed for the nonneutral formula $Nb_2P_3O_{12}$ (i.e., neglecting H and N, and with full occupancies for all atoms), gave a satisfactory profile and bond lengths close to those expected. One distance, however, was then unacceptable (O(2)–O(2) : 2.2 Å). Then the occupancies of Nb and P were fixed at 95.5 and 94%, respectively, according to formula II, thus leading to slightly better R values, to the expected bond lengths, and to the calculated profile shown in Fig. 1. Table 2 summarizes the results.

As the occupancies of Nb and P sites are strongly correlated to the B values, they were refined, as a check, for various fixed values of the thermal B parameters (range 0.4–0.8 Å^2). The resulting occupancies are then in the ranges 93.0(5)–96.0(5)% for Nb, and 88(1)–91(1)% for P(1) and P(2), thus confirming occurrence of the vacancies. These refined occupancy values are, in the case of P, still lower than those expected. However, the O(2)–O(2) distance is once again unsatisfactory, and the improvement in R very weak. Consequently, considering both the R values and the interatomic distances, the best results are those given in Table 2, which corresponds to the occupancies inferred from the chemical analyses. The final Fourier-difference map has maxima and minima in the range ±3.7 e/Å^3. Although precise values of the vacancy concentrations are not obtained, all the results are satisfactory and consistent with formula II.

DESCRIPTION OF THE DEFECT STRUCTURE

A detailed description of the $Sc_2(WO_4)_3$-type structure (7) has been given previously in (9), where the $M_2(XO_4)_3$ framework is compared to that in related types (including Nasicon). Figure 2 illustrates the linking between the polyhedra: each oxygen atom is bonded to a Nb atom and to a P atom, and the three-dimensional framework consists of NbO_6 octahedra and PO_4 tetrahedra sharing all their vertices. Selected bond distances and angles are given in Table 3, where the values (they are mean values since defects exist) are in good agreement with the crystal chemistry of Nb^V phosphates and oxophosphates. These results show fairly regular polyhedra and do not reflect the occurrence of vacancies.

It is difficult to imagine the cation vacancies, in such a structure, without a significant shift of the oxygen atoms surrounding the defects. Let us call such oxygen atoms "terminal oxygen" (O_t). A Nb vacancy and a P vacancy imply six P–O_t bonds and four Nb–O_t bonds, respectively, so that 18% of P forms a P–O_t bond, and 36% of Nb forms a Nb–O_t bond. A great number of examples show that P–O_t bonds are shorter than the other P–O bonds (about 1.48 instead of 1.53 Å), so that O_t–O_t distances close to 2.85 Å are expected around a Nb vacancy. Similarly, Nb–O_t bonds are shorter than Nb–O ··· P bonds (about 1.75, or less, instead of 1.98 Å—see for instance (3, 10)), which leads to O_t–O_t distances close to 2.87 Å, or more, around a P vacancy. Consequently, distances compatible with stability are obtained, and protons trapped at the defects could reinforce the stability via hydrogen bonds.

In order to obtain more direct proof supporting existence of Nb–O_t and P–O_t bonds, and thereby of the vacancies, it was of interest to carry out comparative spectroscopic studies of the title compound and of $Nb_3(NbO)_2(PO_4)_7$, since the latter, with the formula $Nb_2P_{2.8}O_{12}$, also involves short Nb–O and P–O bonds among "normal" bonds (3). Moreover, in both compounds, short and normal bonds occur with approximately the same frequency, and both structures are modifications of the $Sc_2(WO_4)_3$ type. Note that, in the case of $Nb_3(NbO)_2(PO_4)_7$, the short P–O bonds are not P–O_t bonds, but arise from a P–O ··· Nb–O_t linking, where O ··· Nb stands for a weak bond (3). A similar linking probably exists in the title compound as a secondary consequence of the P vacancies, thus leading to similar short P–O or P–O_t: normal P–O ratios in both compounds.

Both $Nb_{2-x}P_{3-y}O_{12}$ and $Nb_3(NbO)_2(PO_4)_7$ being modifications of the same structure, with very similar b and c unit-cell parameters, one can imagine compounds corre-

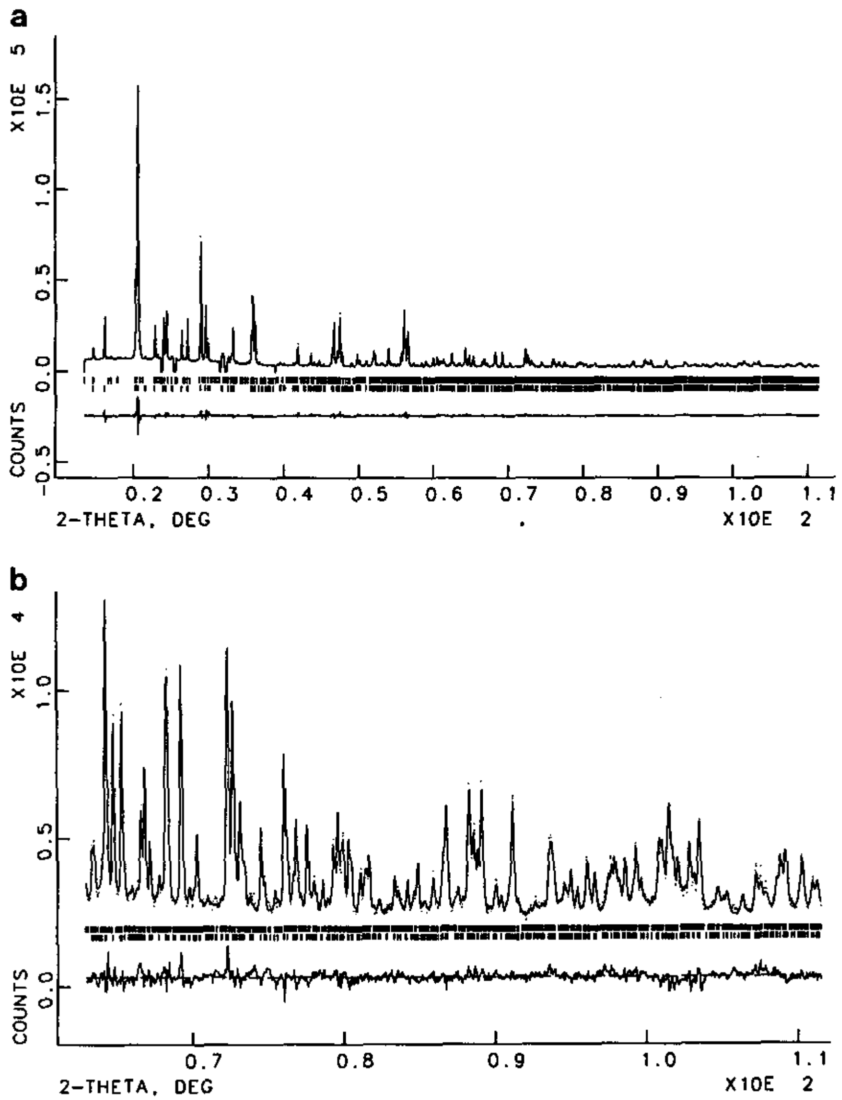

FIG. 1. Observed (···), calculated (—), and difference (same scale) profiles: (a) whole pattern, (b) high angle region.

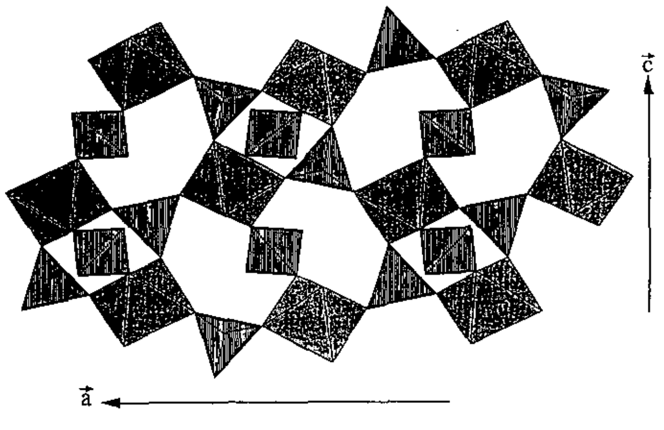

FIG. 2. [010] view of a fragment (upper part) of the unit-cell.

sponding to an intergrowth of these structures. The resulting model would involve both point defects (vacancies) and (100) planar defects (from $Nb_3(NbO)_2(PO_4)_7$). The electron diffraction technique, which is very sensitive to any occurrence of stacking faults, did not indicate such a phenomenon in the title compound.

SPECTROSCOPIC STUDIES

Infrared and Raman Spectra

For both $Nb_{2-x}P_{3-y}O_{12}$ (A) and $Nb_3(NbO)_2(PO_4)_7$ (B), Raman spectra were taken in the range 280–1500 cm^{-1}, using a MICRODIL 28 spectrometer (unpolarized incident beam, SPECTRA PHYSICS 2000 argon ion laser), and IR spectra were taken in the range 400–4000 cm^{-1}, by KBr method, using a FT-IR NICOLET 20 SX system.

TABLE 3
Selected Interatomic Distances (Å) and Angles (°)

NbO_6 octahedron ⟨Nb–O⟩ = 1.968

Nb	O(1)	O(2)	O(3)	O(4)	O(5)	O(6)
O(1)	1.938(9)	2.74 (1)	2.76 (1)	3.92 (1)	2.72 (1)	2.86(1)
O(2)	89.0 (4)	1.969(9)	2.80 (1)	2.76 (1)	2.75 (1)	3.95(1)
O(3)	89.8 (5)	90.8 (4)	1.971(9)	2.89 (1)	3.93 (1)	2.77(1)
O(4)	175.8 (5)	88.6 (4)	93.7 (4)	1.984(9)	2.74 (1)	2.78(1)
O(5)	88.3 (4)	88.6 (3)	178.0 (4)	88.2 (4)	1.961(9)	2.83(1)
O(6)	93.4 (4)	177.6 (4)	88.9 (4)	89.0 (4)	91.8 (4)	1.99(1)

$P(1)O_4$ tetrahedron ⟨P(1)–O⟩ = 1.52

P(1)	O(2)	O(2)	O(4)	O(4)
O(2)	1.51(1)	2.39(2)	2.52 (1)	2.46 (1)
O(2)	104.5 (9)	1.51(1)	2.46 (1)	2.52 (1)
O(4)	112.1 (5)	108.2 (4)	1.527(9)	2.52 (2)
O(4)	108.2 (4)	112.1 (5)	111.5 (8)	1.527(9)

$P(2)O_4$ tetrahedron ⟨P(2)–O⟩ = 1.53

P(2)	O(1)	O(3)	O(5)	O(6)
O(1)	1.558(9)	2.54(1)	2.54(1)	2.49(1)
O(3)	110.6 (6)	1.53(1)	2.42(1)	2.51(1)
O(5)	110.7 (6)	104.3 (5)	1.53(1)	2.52(1)
O(6)	108.4 (6)	110.9 (7)	112.0 (6)	1.51(1)

Figures 3 and 4 show that compounds A and B possess very similar spectra. In the Raman spectra, the significant difference concerns the band widths, which are greater for the disordered compound, as expected; the differences in band position and intensity are very small. The same is true for the IR spectra, where the major differences concern the intensity of the weak bands in the range 540–650 cm^{-1}.

In the present case, two regions are of particular interest. The bands in the first region, from 1250 to 1300 cm^{-1}, can be unambiguously assigned to stretching of short P–O bonds, so that existence of bands at 1262 and 1281 cm^{-1} (for B) and 1260 and 1275 cm^{-1} (for A) supports the occurrence of a significant number of Nb vacancies in A. The second region of interest, for the short $Nb–O_t$ bonds, would be from 850 to 950 cm^{-1}. Since this region could also concern PO_4 vibrations, one can only assume that the bands at 886 (A) and 884 cm^{-1} (B) in IR spectra arise from $Nb–O_t$ stretching. Nevertheless, since this stretching produces a strong band in Raman spectra around 900 cm^{-1} (11, 12), and since similar bands are observed for A and B in this domain, the spectra also support existence of short $Nb–O_t$ bonds, and thus of P vacancies in A.

Note that a very weak band is seen at 3020 cm^{-1}, so that the weak band at 1450 cm^{-1} in the IR spectrum for A can be assigned to H–N–H bending; therefore, a part of N and H, at least, occurs as NH_4^+ species in A.

MAS NMR spectra

The NMR spectra have been acquired on a Bruker MSL 400 spectrometer, using a Bruker 4-mm high speed probehead spinning at 10 kHz for ^{31}P and 15 kHz for ^{1}H. The pulse length used for ^{31}P is 2 μsec, i.e., ca. 45° for the pulse angle, and for ^{1}H 1 μsec, i.e., ca. 22° for the

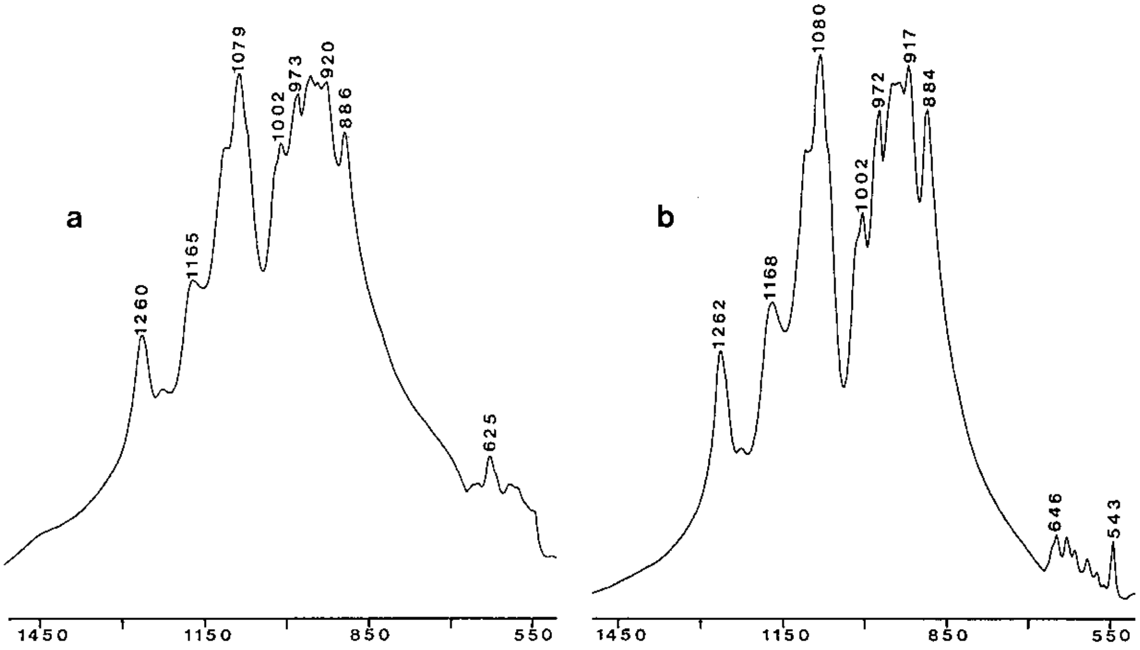

FIG. 3. IR spectra for $Nb_{2-x}P_{3-y}O_{12}$ (a), and $Nb_3(NbO)_2(PO_4)_7$ (b).

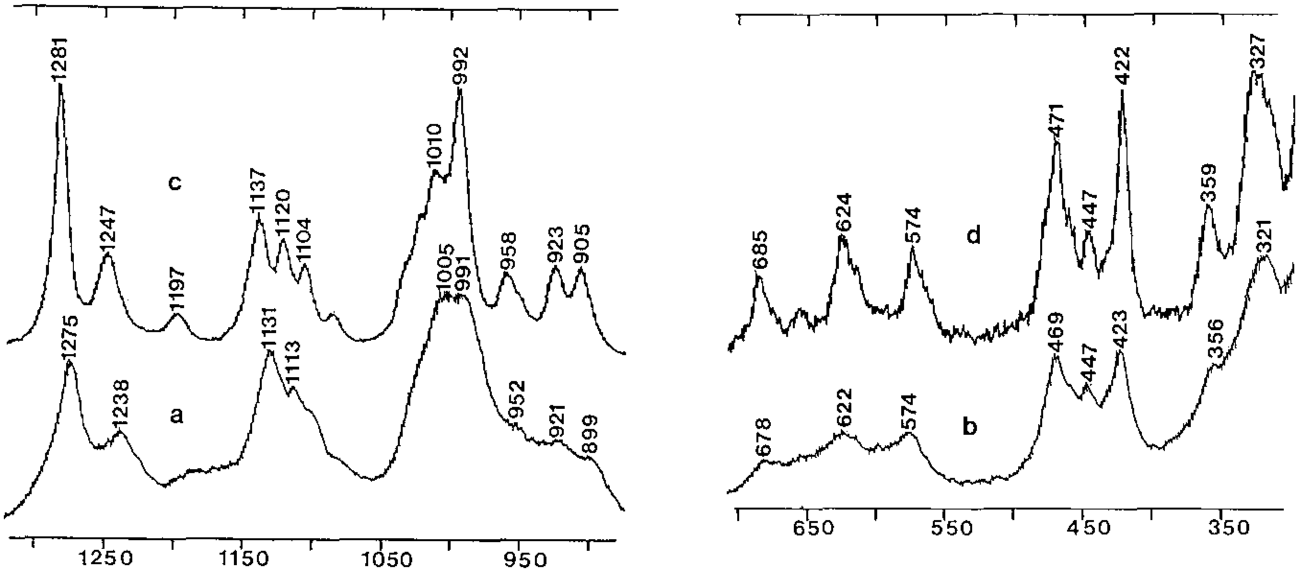

FIG. 4. Raman spectra for $Nb_{2-x}P_{3-y}O_{12}$ (a), (b), and $Nb_3(NbO)_2(PO_4)_7$ (c), (d) (intensities with arbitrary units).

pulse angle. The magnetic field is 9.39 T and the resonating frequency 162 MHz for ^{31}P and 400 MHz for ^1H. The samples are referenced to the 85% H_3PO_4 for ^{31}P and tetramethylsilane for ^1H.

Figure 5 shows ^{31}P MAS NMR spectra for A and B. B contains four independent P atoms (one of them with a short P–O bond), with mean distances of 1.51 and 1.52 Å (3), which lead to a single NMR signal at −27.1 ppm. The mean distance difference does not exceed 0.01 Å. The line width is of 11 ppm. For the title compound A, the spectrum is very similar, with the central line at −27.6 ppm with the same linewidth. The mean P–O distances around the two P are 1.52 and 1.53 Å, differing by no more than ca. 0.01 Å, and additional inequivalent P atoms are expected near vacancies.

With the above mean distances, the difference on the isotropic chemical shift of phosphorus is expected not to exceed 12 ppm in each structure. With an overall

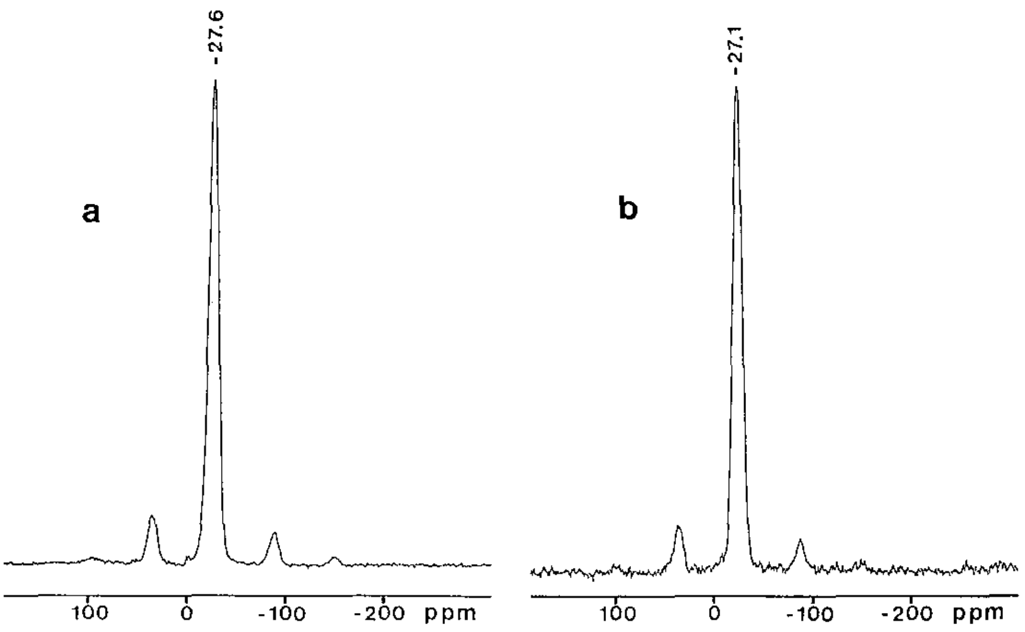

FIG. 5. ^{31}P MAS NMR spectra for $Nb_{2-x}P_{3-y}O_{12}$ (a) and $Nb_3(NbO)_2(PO_4)_7$ (b).

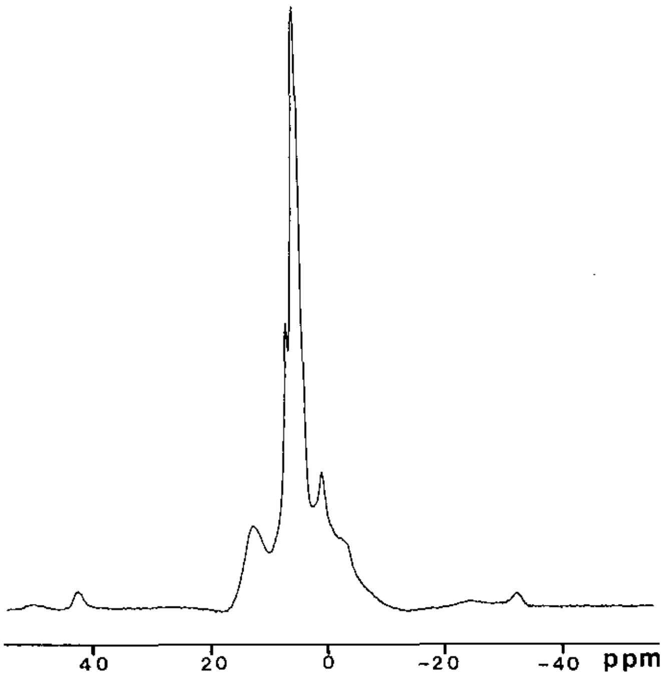

FIG. 6. ^1H MAS NMR spectrum for $Nb_{2-x}P_{3-y}O_{12}$.

line width of 11 ppm, the sites are not resolved. Assuming that their chemical shift difference is at its maximum, i.e., 6 ppm, one can expect to get an upper limit for the individual linewidth of ca. 6 ppm, i.e., an isotropic distribution of the mean P–O distance of 0.006 Å.

The two inequivalent phosphorus of the refined structure could have been further differentiated by the niobium vacancies creating P–O_t bonds. The distance distribution, however, is almost identical in the A and B compounds. Therefore, with respect to the situation observed for B, the niobium vacancies do not notably increase the mean P–O distance distribution, which is already large in B and stays at the same value in A.

Figure 6 shows the proton MAS NMR spectrum obtained for A. A comparative study of line intensity ($NH_4NbOP_2O_7$) (4) as standard) indicated that this spectrum agrees with the low H content inferred from the chemical analyses. It can be seen, in Fig. 6, that the protons occur in a variety of states in $Nb_{2-x}P_{3-y}O_{12}$, from basic to acid states, including ones which can be associated to NH_4^+ and H_2O species (lines at 7 and 5 ppm). For the structural model described above, NH_4^+ and H_2O species should be bonded at the surface, and more or less acidic protons are probably trapped at the defects, in the bulk, thus lowering their energy.

At this time, the problem of the nitrogen bonding is not fully solved. There is evidence of NH_4^+ occurrence, and, at the same time, the fraction of protons present as NH_4^+ appears very small. Taking into account the N : H atomic ratio obtained (close to 1 : 4), it can be deduced that N also forms other bonding. We suppose the occurrence of nitride.

THERMAL BEHAVIOR

Thermal Behavior in Air

The thermal behavior of $Nb_{2-x}P_{3-y}O_{12}$ was investigated, using XRPD, TGA, and, in some cases, FT-IR measurements.

The TG curves (heating rate of 1.4 K/mn, Perkin–Elmer system) show:

—at low temperature (20–100°C) a small weight loss of approximately 0.3%, which must be associated with surface water molecule loss,

—a small weight loss (approximately 0.4%), between 500 and 700°C, which may corresond to the loss of a part (about 30%) of protonic species in the bulk.

By heating for several days at temperatures in the range 700–900°C, a slight broadening of the XRPD lines is obtained, without significant modification of the IR spectra. Heating for the same time at 950°C leads to α-$NbOPO_4$.

Note that the decomposition is slow, since heating for 5 hr at 1000°C leads to the XRPD pattern of the starting phase, with fairly narrow lines.

Thermal Behavior under Reducing Conditions

The mixed-valence compound $Nb_2(PO_4)_3$ exists, with a Nasicon-like structure (13) and $Nb_2P_3O_{12}$ composition; therefore one can imagine that it could be obtained by reducing the title compound.

$Nb_{2-x}P_{3-y}O_{12}$ was heated under reducing atmosphere (15% H_2, 85% Ar), for 2 days, at 750 or 900°C. For 900°C, partial decomposition occurs, with formation of β-$NbOPO_4$ (mainly) and α-$NbOPO_4$. The treatment at 750°C yields a blue compound, without modification of the XRPD pattern. Magnetic susceptibility measurements in the range 80–300 K show a very weak paramagnetism and a very low Nb^{IV} concentration.

The formation of $Nb_2(PO_4)_3$ with a Nasicon-like structure was not observed, even at 900°C.

COMPARISON WITH PREVIOUS WORK

In Ref. (1), the authors suppose that the compound "Nb_2O_5,$3P_2O_5$,$4H_2O$," which gives $NbP_3O_{10}.2H_2O$ composition, does not correspond to a single phase, so that comparison with the title phase cannot be discussed.

The so-called "ε-$NbOPO_4$" (2), hereafter named "ε," exhibits XRPD data extremely close to those of $Nb_{2-x}P_{3-y}O_{12}$, so that the structure of ε is also closely related with the $Sc_2(WO_4)_3$ type. This is confirmed by comparison of the IR spectra of $Nb_{2-x}P_{3-y}O_{12}$ (Fig. 3(a)) and of ε (2). Both spectra are extremely similar, except in the region 850–950 where ε gives no band. This absence suggests the absence of short Nb–O bonds in ε (in the structure this would correspond to the absence of P vacancies).

Attempts to reproduce the preparation of ε were unsuccessful, even by varying the heating temperature or the Nb : P atomic ratio between 1 : 1 and 2 : 3 for the reactants. Mixtures of phases were always obtained. Other attempts, varying also the starting reactants, were also unsuccessful, so that the existence of ε-$NbOPO_4$ seems questionable. Its basic structure and its formula could be accounted for by a formula such as $Nb_2(P_{2.4}Nb_{0.4}\square_{0.2})O_{12}$, i.e., with P vacancies and tetrahedral Nb. It is difficult, however, to accept these features without a significant variation of the unit-cell parameters and without corresponding features in the IR spectrum.

At this time, there is no experimental evidence for any nonstoichiometry domain for the title phase.

CONCLUSION

Both $Nb_{2-x}P_{3-y}O_{12}$ and $Nb_3(NbO)_2(PO_4)_7$ are oxophosphates closely related to the $Sc_2(WO_4)_3$ type. In the latter, the structure has been described as resulting from ordered P vacancies (3). In the former, both Nb and P desordered vacancies exist, and stabilization from a few protons in the structure is likely.

ACKNOWLEDGMENTS

The authors are grateful to R. Marchand (Rennes University) for the analyses of N. They are very indebted to L. Rabardel (Bordeaux University) for the density measurements.

REFERENCES

1. N. G. Chernorukov, N. P. Egorov, and V. F. Kutsepin, *Zh. Neorg. Khim.* **24,** 1782 (1979).
2. H. Chahboun, D. Groult, and B. Raveau, *C.R. Acad. Sci. Paris Sér. 2* **304,** 807 (1987).
3. J. J. Zah-Letho, A. Jouanneaux, A. N. Fitch, A. Verbaere, Y. Piffard, and M. Tournoux, *Eur. J. Solid State Inorg. Chem.* **29,** 1309 (1992).
4. J. J. Zah-Letho, Thesis, Abidjan, 1993.
5. J. Guyader, F. F. Grekov, R. Marchand, and J. Lang, *Rev. Chim. Miner.* **15,** 431 (1978).
6. A. Jouanneaux, A. N. Fitch, S. Oyetola, A. Verbaere, D. Guyomard, and Y. Piffard, *Eur. J. Solid State Inorg. Chem.* **30,** 125 (1993).
7. S. C. Abrahams, and J. L. Bernstein, *J. Chem. Phys.* **45,** 2745 (1966).
8. A. C. Larson, and R. B. Von Dreele, "Generalized Structure Analysis System." Los Alamos, 1990.
9. Y. Piffard, A. Verbaere, and M. Kinoshita, *J. Solid State Chem.* **71,** 121 (1987).
10. M. Fakhfakh, S. Oyetola, N. Jouini, A. Verbaere, and Y. Piffard, *Mat. Res. Bull.* **29,** 97 (1994).
11. J. M. Jehng, and I. E. Wachs, *Chem. Mater.* **3,** 100 (1991).
12. G. T. Stranford, and R. A. Condrate, *J. Solid State Chem.* **52,** 248 (1984).
13. A. Leclaire, M. M. Borel, A. Grandin, and B. Raveau, *Acta Crystallogr. Ser. C* **45,** 699 (1989).